第25回橋梁等の耐震設計シンポジウム
講演論文集（2022年7月）

Analytical Study on the Factors Affecting the Seismic Response of Cu-Based SMA Reinforced Concrete Bridge Columns

Rie Bamba[1]・Hartanto Wibowo[2]・Sri Sritharan[3]・Koji Kinoshita[4]

[1]Student Member of JSCE, Department of Civil and Environmental Engineering, Gifu University （1-1 Yanagido, Gifu City 501-1193, Japan）
[2] Assistant Teaching Professor, Department of Civil, Construction & Environmental Engineering, Iowa State University (813 Bissell Road, Ames, IA 50011)
[3] Assistant Dean for Research and Wilkinson Chair Professor of Interdisciplinary Engineering, Department of Civil, Construction & Environmental Engineering, Iowa State University (813 Bissell Road, Ames, IA 50011)
[4] Member of JSCE, Associate Professor, Department of Civil Engineering, Gifu University（1-1 Yanagido, Gifu City 501-1193, Japan）

1. Introduction

In a typical seismic design, conventional reinforced concrete bridge columns are expected to undergo large plastic deformations under a severe earthquake event to dissipate the seismic energy. This often leads to significant residual displacements that in turn prevent the bridge from being operable after the earthquake. As an alternative design solution, shape memory alloys (SMAs) can be used to replace the steel rebars in the critical plastic hinge regions. SMAs have a unique superelastic characteristic that will allow it to essentially return to its original shape after experiencing a large inelastic deformation, thus significantly reducing the residual displacement. The most widely used SMA is Nitinol, which consists of nickel (Ni) and titanium (Ti), but its high cost hinders its application in civil engineering. Copper (Cu)-based SMAs, which is more cost-effective, has been proposed as rebars in reinforced concrete bridge columns[1)2)]. It has been shown that the behavior of Cu-based SMAs are affected by its compound, the loading rate, and the temperature[1)3)4)]. In this study, a numerical model of a Cu-based SMA reinforced concrete column was developed in OpenSees[5)] and was validated with the experimental results from a test performed by Varela and Saiidi at University of Nevada, Reno[2)]. The developed numerical model was also used to investigate the influence of key factors of SMA that affect the seismic response of bridge columns.

2. Development of the Numerical Model

The shake table test by Varela and Saiidi[2)] is shown in **Fig. 1**. Along with the experimental study, they also developed a 2-dimensional (2D) column model using finite element software OpenSees[5)]. Some improvements to the numerical model were necessary which are discussed herein.

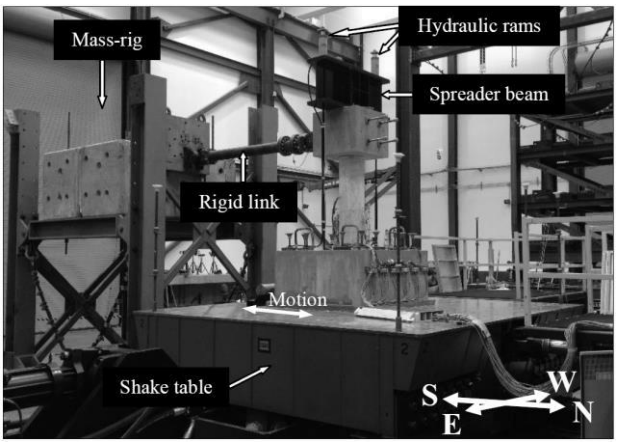

Fig. 1 Shake table test at the University of Nevada, Reno[2)]

(1) Overview of the Specimen Used in the Experimental Study by Varela and Saiidi[2)]

The elevation and cross-sectional views of the ¼-scale column used in the experiment are shown in **Figs. 2** and **3**. The SMA rebars were only placed in the plastic hinge region, as indicated in **Figs. 2** and **3**. Initially, the conventional column was designed in accordance with the AASHTO Specifications[6)]. The column diameter was 14 in. (355.6 mm), and its height was 63.5 in. (1612.9 mm). The column was reinforced with twelve longitudinal rebars in a circular pattern. CuMnAl SMA rebars with a diameter of 0.45 in (11.4 mm) was used within a 10-in. (254-mm) height from the top of the footing, in the plastic hinge region of the column. ASTM A-615 Gr. 60 #5 mild steel rebars with a diameter of 0.625 in (15.875 mm) was used as the longitudinal rebars outside this region and connected to the SMA rebars using 9/16-18 threaded coupling nuts. Each coupler had an engagement length of approximately 1 inch (25.4 mm). The reinforcement ratio

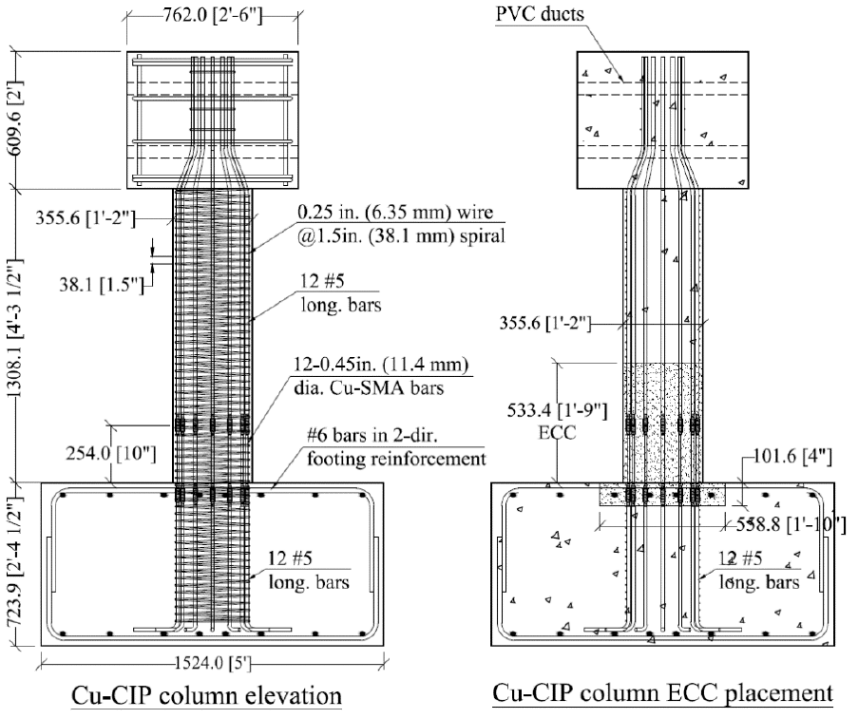

Fig. 2 Elevation views of the tested specimen[2)]

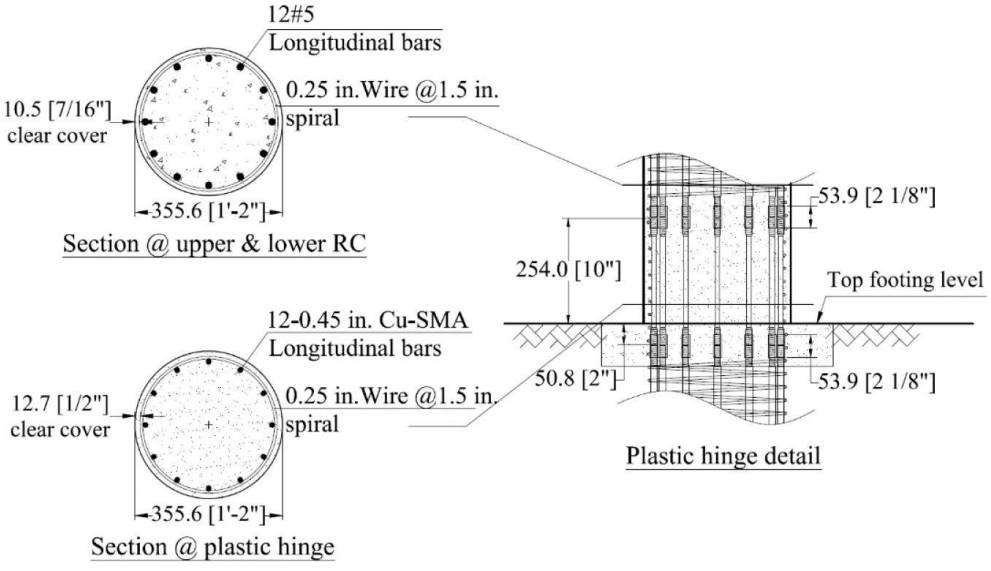

Fig. 3 Cross sections of the tested specimen[2)]

was equal to 2.4% at the upper part where steel rebars were used and 1.2% at the lower part where SMA rebars were used. However, the yield stress of the steel rebars were 73.5 ksi (514.5MPa), whereas the yield stress of the SMA rebars were 24 ksi (168MPa). Therefore, the effectiveness of the longitudinal rebar was even lower at the lower part of the column. Along with the conventional concrete, Engineered Cementitious Composite (ECC) concrete was used over the column height of 21 in. (533.4 mm) from the top of the footing. ECC concrete is composed of fine aggregates, Portland cement, particular admixtures, and Polyvinyl Alcohol (PVA) fibers. The fibers make the ECC concrete more ductile in tension and compression, and fibers prevent ECC from experiencing premature spalling. Therefore, ECC can also sustain s the high strains of the SMA rebars and reduce damage in the plastic hinge region. The measured maximum 56-day strength and strain of ECC concrete cylinder samples were 5.6 ksi (39.2 MPa) and 0.0036, respectively. The compressive strength of the conventional concrete on the test day (189 days) was 6.5 ksi (35 MPa).

The 1994 Northridge, California earthquake recorded at the Rinaldi Receiving Station (RRS 228) was selected as the input motion for the test (**Fig. 4**). Since the geometric scaling of the column was 1/4, the scaling for the time in the acceleration record was $1/\sqrt{4}$ to satisfy the similitude requirements. The design earthquake (DE) level was calculated according to the 2009 AASHTO Guide Specifications for LRFD Seismic Bridge Design[7]. This corresponds to a spectral acceleration value of 0.290 g. To achieve a column drift of up to about 7 to 8%, the load protocol was incremental up to 350% DE as shown in **Table 1**, which also includes the target and achieved scaling factors, as well as peak ground acceleration (PGA) for each run.

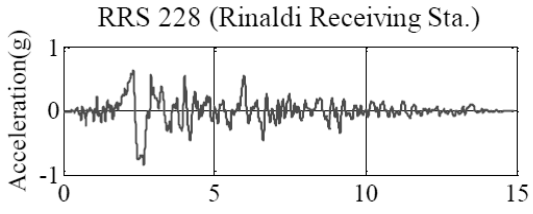

Fig.4 Unscaled acceleration of the input ground motion record[2]

Table 1 Summary of target and achieved ground motions[2]

	Target			Achieved		
Run#	Motion PGA* (g)	x Rinaldi* (RRS 228)	x DE*	Motion PGA (g)	x Rinaldi (RRS 228)	x DE
1	0.073	0.087	25%	0.078	0.094	27%
2	0.145	0.173	50%	0.167	0.199	57%
3	0.290	0.346	100%	0.352	0.420	121%
4	0.435	0.520	150%	0.543	0.649	187%
5	0.580	0.693	200%	0.735	0.878	254%
6	0.871	1.039	300%	1.134	1.353	391%
7	1.016	1.212	350%	1.314	1.569	453%

PGA*: Peak ground acceleration
x Rinaldi*: scaling factor
100% x DE*: Design spectral acceleration

(2) Overview of the Numerical Model Used by Varela and Saiidi[2]

The 2D model developed by Varela and Saiidi[2] is shown in **Fig. 5,** which also has information on the element types, section types, and uniaxial material models that were selected. The stress-strain relationships incorporated into the material models are shown in **Fig. 6**. The force-based element was used for all two elements modeling the column. Confined concrete propertied were based on the modified Mander's model[8]. For the confined ECC concrete properties, the model by Motaref et al.[9] was used. Furthermore, confined concrete was modeled by UniaxialMaterial Concrete04, while unconfined concrete and ECC concrete were modeled by UniaxialMaterial

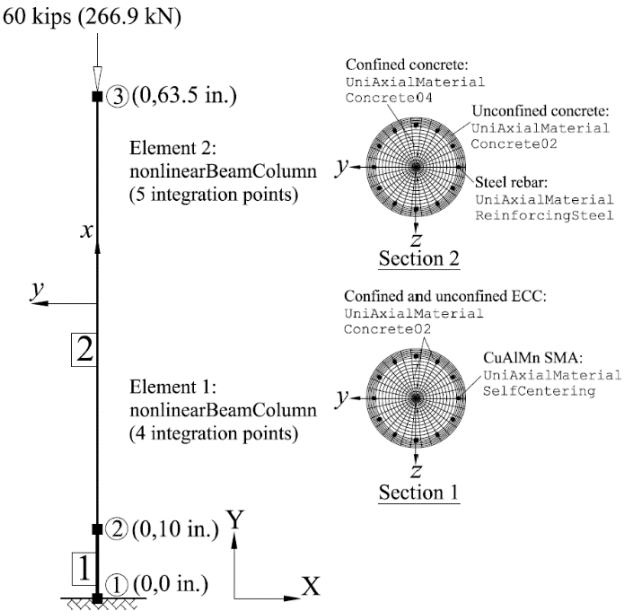

Fig. 5 Geometry of the previous analytical model [2]

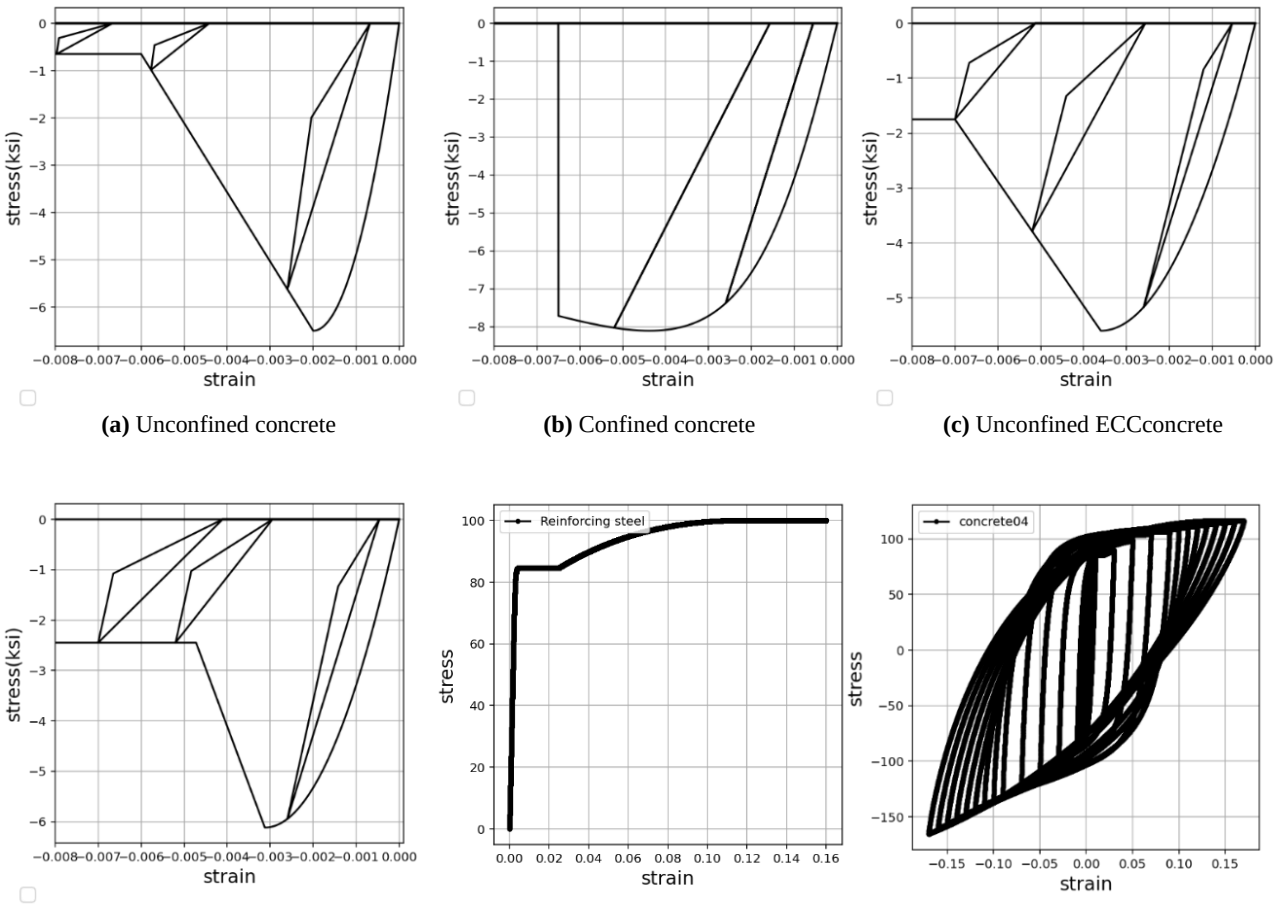

(a) Unconfined concrete **(b)** Confined concrete **(c)** Unconfined ECCconcrete

(d) Confined ECCconcrete **(e)** Reinforcing steel tensile **(f)** Reinforcing steel cyclic

Fig. 6 The constitutional model corresponding to of each material[2)]

Concrete02 (Kent-Scott-Park model) with no tensile strength. Steel rebars were modeled using UniaxialMaterial ReinforcingSteel following the model by Chang and Mander[10)]. A flag-shaped material model by Christopoulos et al.[11)] (UniaxialMaterial SelfCentering) was used to capture the SMA behavior. The model was initially developed to capture a self-centering energy dissipative brace but had also been adopted for SMA rebars. The constitutive SMA model is shown in **Fig. 7**. When the SMA rebar is loaded, it yields at σ_y and the slope changes from k_1 to k_2. Futhermore, when unloaded, the SMA is subjected to back stress($\beta*\sigma_y$) and return to its original shape with slopes of k_2 and k_1. To adjust the ratio of forwarding to a reverse stress, the β factor was used. From the tensile test results of the CuAlMn SMA sample bar, the β factor was 0.20. Nevertheless, β factor of 0.50 (**Fig. 8**) was used for the numerical analysis results to match to the experimental results, without adequate explanations. The other parameters of the flag shape model obtained from the tensile test are shown in **Table 2**.

(3) Improvements to the Numerical Model

To improve results from the numerical model, three changes were made. First, the β factor of 0.50 was changed to remain close to the result from the SMA sample bar test. Sincethe last loop of the cyclic test was unstable, the second last loop from the test was used to determine the value of the β factor, which was 0.32 (**Figs. 9** and **10**). Second, strain penetration effects were included to capture rebars slipping relative to the surrounding concrete under tensile forces, which impact the local and global responses. To achieve this, the mild steel rebars were modeled the zero-length section using the Bond_SP01 material[12)] (**Fig. 11**). Third, a new section was added to consider the effect of the coupler. The coupler was expressed as larger steel rebar which is 1.1 in. (27.9 mm) diameter to accurately capture its rigidity.

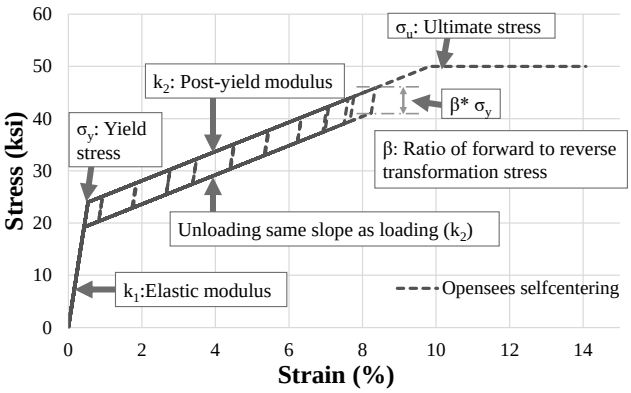

Fig. 7 Constitutive SMA model (SelfCentering Material[11])

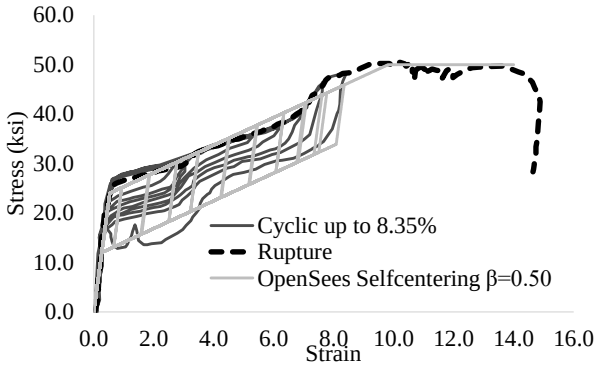

Fig. 8 CuMnAl SMA rebar tensile test[2] and Constitutive model response comparison

Table 2 Parameters of flag shaped model from the tensile test[2]

Elastic modulus	Post-yield modulus	Yield stress	Ultimate stress	Ratio of forward to reverse transformation	Rupture strain
k_1, ksi [MPa]	k_2, ksi [MPa]	σ_y, ksi [MPa]	σ_u, ksi [MPa]	β	ε_u
4500 [31.5]	280 [19.6]	24 [168]	50 [350]	0.20	0.14

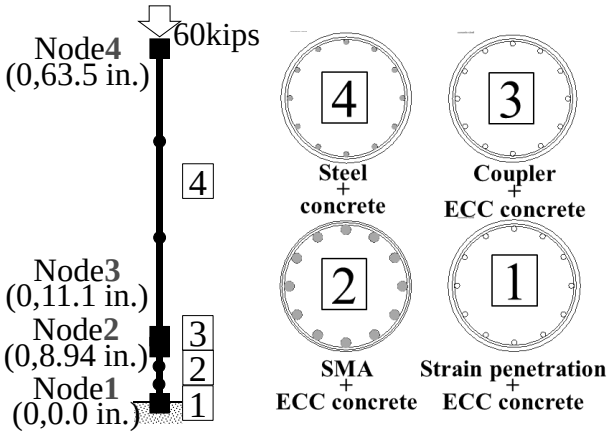

Fig. 9 Improved analytical model

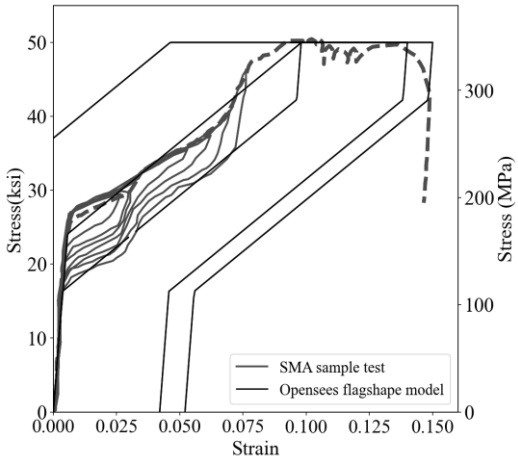

Fig. 10 Self-centering model with β=0.32

3. Numerical Validation

Fig. 12 shows the comparison of the hysteresis loops between the experimental results, the results from the numerical analysis of Varela and Saiidi's model, and those from the improved model for Runs 7. In each figure, **(a)**, **(b)**, **(c)**, **(d)** ,and **(e)** the comparison of the results obtained from the model reproduced from Varela and Saiidi's study, the model when only the coupler used, the model when only the β value was changed from 0.50 to 0.32, and the model when strain penetration effects and the bond bond-slip associated with strain penetration was included, and

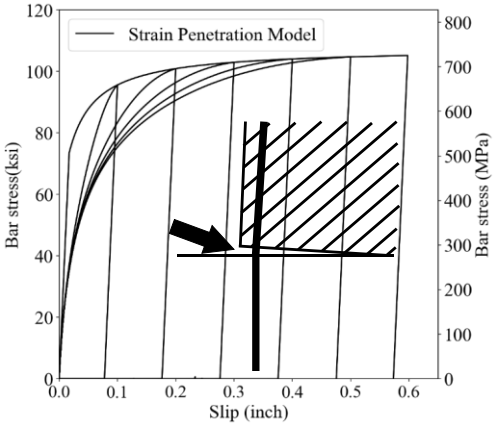

Fig. 11 Strain penetration model[12]

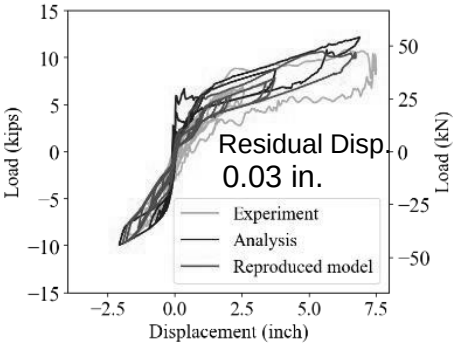

(a) Reproduce model of Varel and Saiidi's

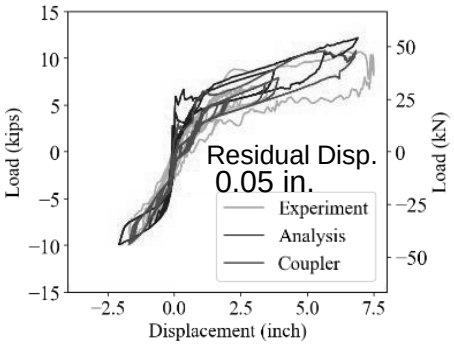

(b) Adding only the effects of couplers

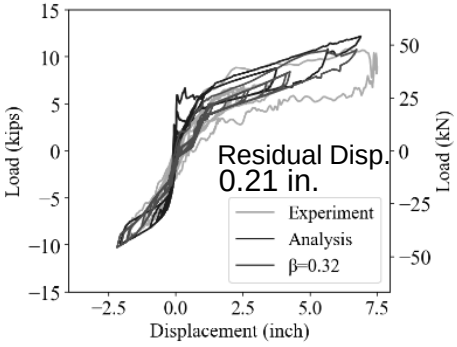

(c) β value changed from 0.50 to 0.32

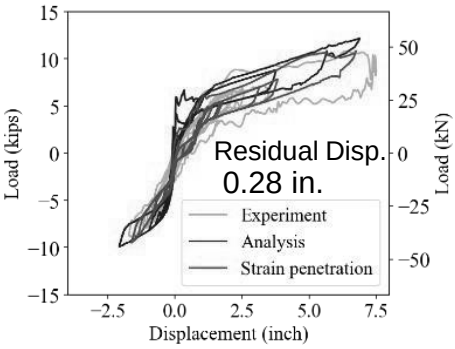

(d) Adding strain penetration effects

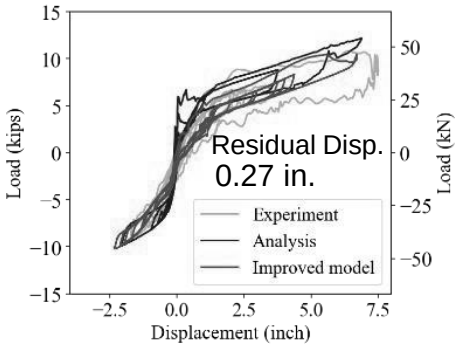

(e) Adding coupler, β=0.32, Adding strain penetration

Fig. 12 Hysteresis response for at Run7

the model that incorporated all three changes, respectively. When the couplers were added to the conventional model, the maximum displacement was diminished on the negative side of the displacement, which is closer to the experimental results than the previous model. This is believed to be due to the stiffness of the columns being slightly increased due to incorporating the couplers. Similarly, the use of the strain penetration model did not make a significant difference in Runs 1-6, but it positively impacted the load displacement on the negative side of displacement for Run 7. This is considered to be due to the fact that the addition of strain penetration effects reduced the concentration of strain and some reduction to the moment resistance at the base of the columns. On the other hand, when the β value was changed, the unloading rate of the stress-strain curve of SMA rebar became smaller, resulting in a thinner hysteresis loop for the column response. This result indicates that the previous model developed by Varela and Saiidi overestimated the hysteresis loops of the column response.

The selected results of the experiment, the numerical analysis by the previous model[2], as well as the numerical analysis by the improved model, which incorporated the aforementioned refinements, are summarized in **Fig. 13**. According to the graphs, maximum load and maximum displacement are in good agreement with results from the

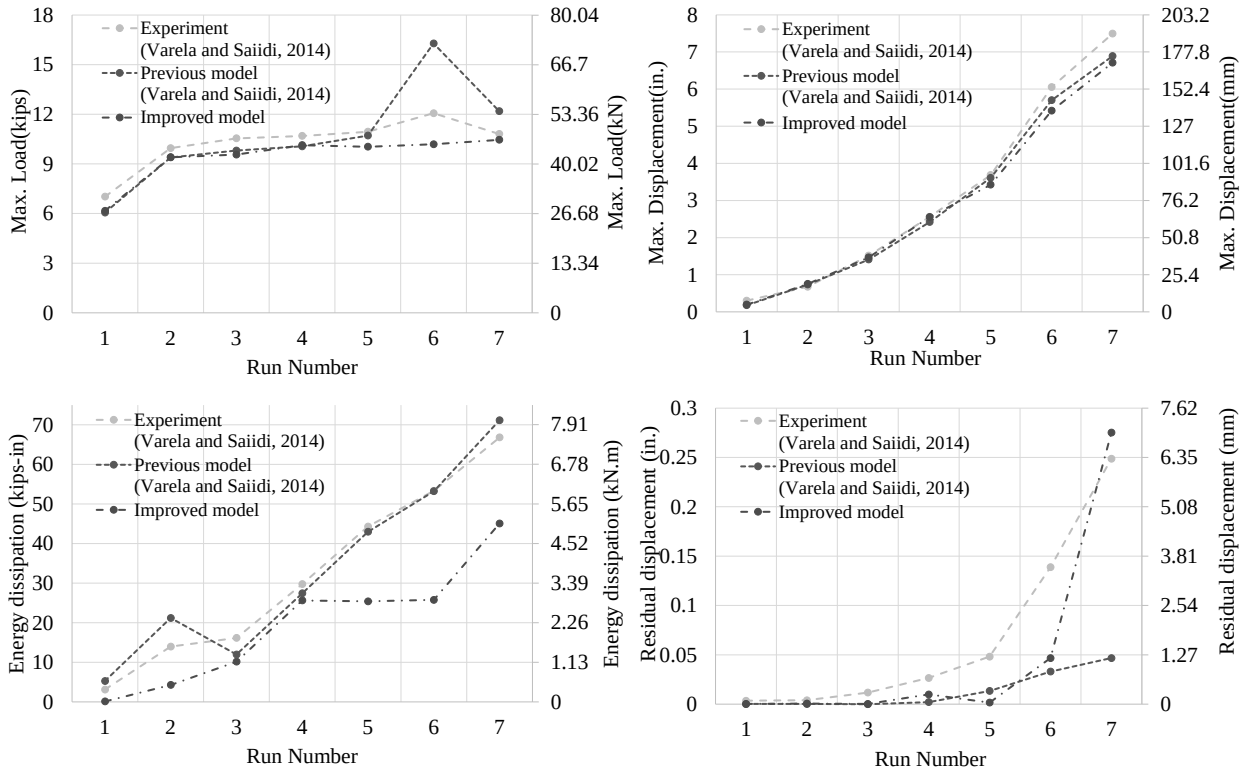

Fig. 13 Comparison of key results for various runs

experiment. Overall, the residual displacement is slightly small, but for run7, it is in good agreement with the experimental results. Because of the smaller β factor and incorporation of strain penetration effects, the residual displacements were increased. In terms of energy dissipation, the results were not as close as the results from the previous model to the experiment even though the improved model more accurately captured the material behavior. β factor reduced the energy dissipation in the improved model. As a result of closely reproducing, the results were in good agreement with the experimental results in terms of maximum load, displacement, and residual displacement.

4. Conclusions

A numerical model of Cu-based SMA reinforced concrete column was developed using finite element software OpenSees[5], and compared to the results from a test conducted by Varela and Saiidi[2]. The analytical model introduced three new features compared to the model developed by Varela and Saiidi:

1) A new section was added to incorporate the effect of couplers between SMA rebars and steel rebars. Consequently, the maximum displacement on the negative side was decreased which was overestimated by the previous model.
2) Strain penetration effects of the steel longitudinal rebars at the top of the footing were included to capture rebars slipping relative to the surrounding concrete under large tensile stress. As a result, the peak values of horizontal load and displacement were not overestimated.
3) The β value which is the ratio of forwarding to reverse stress for SMA rebars was changed from 0.50 to 0.32 to closely match the results from the SMA sample bar test. It reduced the energy dissipation capacity of the column. These results indicated the previous model overestimated the energy dissipation by SMA rebars.

When the numerical model was improved with these three features, the maximum load, maximum displacement, and residual displacement were in better agreement with experimental values. Consequently, the

improved numerical model can be used to investigate other factors that affect seismic response of bridge columns designed with SMA rebars.

References

1) Geniture B, Hosseini SF.: Use of Cu-based superelastic alloys for innovative design of reinforced concrete columns, *Proceedings of tenth U.S. national conference on earthquake engineering, frontiers of earthquake engineering*, Anchorage, Alaska, 2014.
2) Varela, S., and M. Saiidi: Dynamic performance of novel bridge columns with superelastic CuAlMn shape memory alloy and ECC., *International Journal of Bridge Engineering (IJBE)*, Vol. 2, No. 3, pp. 29-58, 2014.
3) Y. Araki, T. Endo, T. Omori, Y. Sutou, Y. Koetaka, R. Kainuma, K. Ishida: Potential of superelastic Cu–Al–Mn alloy bars for seismic applications, *Earthq. Eng. Struct. Dyn*., Vol.40, No.1, pp. 107-115, 2011.
4) B. Gencturk, Y. Araki, T. Kusama, T. Omori, R. Kainuma, F. Medina: Loading rate and temperature dependency of superelastic Cu–Al–Mn alloys, *Constr Build Mater*, Vol.53, pp. 555-560, 2014.
5) Mazzoni, S., McKenna, F., Scott, M.H., Fenves, G.L.: OpenSees Command Language Manual, Berkeley, CA, 2006.
6) AASHTO: AASHTO Guide Specifications for LRFD Seismic Bridge Design, American Association of State Highway and Transportation Officials, Washington, DC, 2011
7) AASHTO: AASHTO Guide Specifications for LRFD Seismic Bridge Design, American Association of State Highway and Transportation Officials, Washington, DC, 2009
8) Mander, J. B., Priestly, M. J. N. and Park, R.: Theoretical stress-strain model for confined concrete, *ASCE J. Struct*. Engng Vol.114, No.8, pp.1804-1826, 1988.
9) Motaref, S., Saiidi, M., and Sanders, D.: Seismic response of bridge columns with energy dissipating joints, Center for Civil Engineering Earthquake Research, Department of Civil and Environmental Engineering, University of Nevada, Reno, Nevada, Report No. CCEER-11-01, 2011.
10) Chang, G., and Mander, J.: Seismic energy based fatigue damage analysis of bridge columns: Part I- Evaluation of seismic capacity, *NCEER Report 94-0006*, State University at Buffalo, NY, 1994.
11) Christopoulos, C., Tremblay, R., Kim, H., and Lacerte, M.: Self-Centering Energy Dissipative Bracing System for the Seismic Resistance of Structures: Development and Validation, *ASCE Journal of Structural Engineering*, Vol. 134, No.1, pp. 96-107, 2008.
12) Zhao, J., and S. Sritharan.: Modeling of strain penetration effects in fiber-based analysis of reinforced concrete structures. *ACI Structural Journal*, 104(2), pp. 133-141, 2007.